THE ASTROPHYSICAL JOURNAL, 362:241–250, 1990 October 10

ELECTRON CAPTURE AND β-DECAY IN PRESUPERNOVA STARS

M. B. AUFDERHEIDE
Physics Department, State University of New York at Stony Brook; and Department of Physics, Brookhaven National Laboratory
G. E. BROWN, T. T. S. KUO, and D. B. STOUT
Physics Department, State University of New York at Stony Brook
AND
P. VOGEL
Physics Department, California Institute of Technology
Received 1989 September 25; accepted 1990 April 2

ABSTRACT

We carry out calculations of electron capture and β-decay from several odd-even and odd-odd nuclei with $A > 60$, seeking the largest transitions. Of these, only the $^{60}\mathrm{Co} + e^- \rightarrow {}^{60}\mathrm{Fe} + \nu_e$ transition has been previously evaluated in a shell model calculation, by Fuller *et al.*, in a form suitable for inclusion in stellar evolution calculations. For neutron-rich stellar cores with $Y_e = Z/A = 0.42$ to 0.43, this single transition accounts for roughly half of the total electron capture in present evolutionary calculations, even though the abundance by mass fraction of $^{60}\mathrm{Co}$ is only on the order of 10^{-5}. We show that nuclei with $A > 60$, essentially not included to date, may make significant contributions to the electron capture and β-decay rates in the last stages of stellar evolution.

Subject headings: nucleosynthesis — stars: supernovae

I. INTRODUCTION

The basis for understanding electron capture during the late stages of stellar evolution was formulated by Bethe *et al.* (1979, hereafter BBAL). These authors used the reaction $^{56}\mathrm{Fe}(e^-, \nu_e)\,{}^{56}\mathrm{Mn}$ with a zero-order shell model to point out that considerable Gamow-Teller strength should be present at excitation energies of a few MeV in the daughter nucleus $^{56}\mathrm{Mn}$, and thus the continuum electron capture rate should be rapid in the presupernova stellar collapse where electron Fermi energies reach several MeV. Fuller, Fowler, and Newman (hereafter FFN) with similar shell model techniques, made estimates of Gamow-Teller resonance strengths and energy centroids which were then employed with the available experimentally determined energy levels and *ft*-values to compute nuclear reaction rates over a broad range of nuclei and stellar conditions (FFN 1980*a*, *b*, and 1985).

The FFN calculations were carried out for both the "electron capture direction" and the "positron capture direction." The former includes both continuum electron capture and β^+-decay, while the latter includes β^--decay and continuum positron capture. The "electron capture direction," or $T^< \rightarrow T^>$ transitions, can be explored experimentally by (n, p) experiments. Such recent experiments (Häusser and Vetterli 1988) have shown the extensive Bloom and Fuller calculation (1985) to be basically correct, but determine an empirical quenching factor, similar to those known for (p, n) reactions, which should be applied. Part of such a quenching factor arises from truncation of shell model calculations to the lowest shells and selected configurations. But there remains a residual factor of ~ 0.6, which takes into account the strength that has been moved quite far upward in energy by tensor interactions (Bertsch and Hamamoto 1983), and strength moved even further into the $\Delta(1230)$ isobar region (Bohr and Mottleson 1981; Brown and Rho 1981).

In the most naive shell model calculation which we shall use in this paper, the quenching factor for the $^{54}\mathrm{Fe} \rightarrow {}^{54}\mathrm{Mn}$ transition is (Häusser and Vetterli 1988) $\lesssim 0.35$. With the more extensive Bloom and Fuller calculation (1985), the factor is ~ 0.4.

In this paper we wish to extend the work of FFN to $A > 60$. It was shown in BBAL that, as a result of electron capture, the average number of nucleons per nucleus ($\bar{A}$) moves upward. The work of BBAL pertained to higher densities and temperatures than are relevant in the precollapse evolution of stars, and these authors averaged over pairing gaps, a procedure which was justified only for their higher temperatures ($T \gtrsim 8 \times 10^9$ K). In the precollapse evolution where temperatures are lower (2×10^9 K $< T < 5 \times 10^9$ K), the nuclear effects of odd-odd compared with even-even nuclei can make quite a difference. As a result, the relevant $\hat{\mu}$'s are less than half those tabulated in BBAL. Here $\hat{\mu} \equiv \mu_n - \mu_p$, where μ_n and μ_p are neutron and proton chemical potentials, respectively. Because the BBAL $\hat{\mu}$'s are too large, the $\bar{A}$'s computed there will not be quantitatively accurate. Nonetheless, there is a tendency for $\bar{A}$ to increase with decreasing Y_e. Here Y_e is the ratio of the number of electrons to the number of nucleons. Since we consider conditions in which essentially all nucleons are in nuclei, T_e is simply given by

$$Y_e = \left\langle \frac{Z}{A} \right\rangle . \tag{1}$$

Current stellar evolution calculations predict Y_e's of 0.42–0.43 for the center of the 18 $M_\odot$ (Woosley, Pinto, and Weaver 1988) star appropriate for the progenitor of SN 1987A, and this is on the edge of the FFN matrix of nuclei. Clearly, additional rates for the higher A nuclei will allow more electron capture.

It is also true that β-decays for these nuclei have been neglected. The net effect of these reactions is to increase the value of Y_e. Thus both electron capture and β-decay rates must be calculated if we are to see the full effects on the value of Y_e.

Electron capture and β-decay rates for the allowed Gamow-

Teller transitions exceed those for the forbidden ones by orders of magnitude, so we consider in this paper only allowed transitions. First, we calculate the $^{60}\mathrm{Co} + e^- \rightarrow {}^{60}\mathrm{Fe} + \nu_e$ reaction and compare it to the FFN result, since it has played such a large role in electron capture to date. Then we extend the calculations to the higher A cobalt isotopes and some of the copper isotopes. We then consider some of the large β-decays in this range of A.

In this paper, we calculate transitions from only the lowest state of the parent nucleus having an allowed transition. Usually we can connect these with a measured transition. It is clear that we underestimate the total transition strength. Extensive shell model calculations will be needed to indicate how much strength lies in excited levels. Furthermore, (n, p) measurements (Häusser and Vetterli 1988) are being extended to other nuclei, so we should reach a better understanding of strength in the higher levels soon.

These reactions do not go down a chain of nuclei in the presupernova environment. Nuclear statistical equilibrium is maintained by the strong and electromagnetic interactions at all times after the completion of silicon burning in the stellar core. We show that the abundances in the Cu region are larger than those in the Co region, in accord with the arguments of BBAL. However, quenching factors are somewhat smaller.

The Cu region is substantially more favorable for electron capture than the Co one, because the allowed Gamow-Teller transitions go from the ground states in the former cases. Except for ^{64}Co, the transitions are from excited states in the Co region.

Our plan in this paper is to make calculations of some selected rates which look large, in order to show how the nuclear physics can be tied down from experiment. At the same time, one of us (M.B.A.) is formulating the results so that they can be incorporated into stellar evolution calculations.

II. THE $\mathrm{Co} + e^- \rightarrow \mathrm{Fe}$ ELECTRON CAPTURE RATES

In computing such rates, we are interested in the allowed Gamow-Teller transitions between a mother and daughter nucleus in either their ground states or excited states. The energy balance for such a reaction can be written as

$$\epsilon_e + \Delta^* = \hat{\mu} + \epsilon_\nu \,, \tag{2}$$

where ϵ_e and ϵ_ν are the electron and neutrino energies, respectively, $\hat{\mu}$ is the difference in energy between the ground states of the daughter and mother nuclei; Δ^* is the difference in the excitation energies of the mother and daughter nuclei. The rate of an allowed Gamow-Teller transition from one state to another is given ($\hbar = c = 1$ throughout this paper) by

$$\lambda = \frac{G_F^2}{2\pi}\left(\frac{g_A}{g_V}\right)^2 \mathcal{Q}\,|\langle\boldsymbol{\sigma}\rangle|^2 \rho N_A Y_e \frac{(2J_i^{ex}+1)}{Z_n} \times \exp\left(-E_i^{ex}/k_B T\right)\langle\epsilon_\nu^2\rangle \,, \tag{3}$$

where G_F is the Fermi coupling constant, $g_A/g_V = 1.25$ here, ρ is the density, and N_A is Avogadro's number; J_i^{ex} and E_i^{ex} are the spin and excitation energy of the mother nucleus in its excited state, and Z_n is its nuclear partition function. The quenching factor is given by $\mathcal{Q}$, so that $\mathcal{Q}\,|\langle\boldsymbol{\sigma}\rangle|^2$ is the square of the empirical matrix element. The average of the square of the neutrino energy is given by $\langle\epsilon_\nu^2\rangle$. This average is given by

$$\langle\epsilon_\nu^2\rangle = \frac{1}{\pi^2 \rho N_A Y_e}\int_{\mathcal{L}}^{\infty} \frac{p_e^2(\hat{\mu}^* - \epsilon_e)^2 F(Z,\epsilon_e)\,dp_e}{1 + \exp\left[(\epsilon_e - \mu_e)/k_B T\right]} \,, \tag{4}$$

where $\hat{\mu}^* = \hat{\mu} - \Delta^*$, μ_e is the electron chemical potential, and T is the temperature. $F(Z, \epsilon_e)$ is the Fermi function, which includes the effect of the nuclear Coulomb field on the electron wave function. $\mathcal{L}$ is the lower limit of the electron momentum. For $\hat{\mu}^* \leq m_e$, $\mathcal{L}$ is zero, while for $\hat{\mu}^* > m_e$, $\mathcal{L}$ is $\sqrt{(\hat{\mu}^{*2} - m_e^2)}$. The rest of this section will be devoted to how the various pieces of λ are determined for each transition. First we will discuss how $|\langle\boldsymbol{\sigma}\rangle|^2$, the allowed Gamow-Teller matrix element, is computed. Then we will discuss methods of performing the above phase space integral.

From Lederer and Shirley (1978) one sees that the lowest 1^+ state in ^{60}Co is at 0.74 MeV. Calculations performed with a bare G-matrix calculated from realistic forces place the level at about 2.52 MeV. According to the schematic model (Brown 1971), the energy of the Gamow-Teller state should be lowered in proportion to its strength. Thus, one would expect a quenching factor in the strength of $\sim$0.29. This is in line with the factors Häusser and Vetterli (1988) find; e.g., roughly 0.4 for the Fe $\rightarrow$ Mn transitions.

However, we shall try to obtain the Gamow-Teller strengths [B(GT)] from measured β-decays; i.e., use those for the β^- transitions with detailed balance to obtain those in the electron capture direction. This cannot be done for the $^{60}\mathrm{Co}^*(1^+) \rightarrow {}^{60}\mathrm{Fe}(0^+)$ transition, because the 0.74 MeV state in cobalt lies above the ^{60}Fe ground state in energy. But ^{62}Fe beta decays to the 0.5061 excited 1^+ state of ^{62}Co* essentially 100% of the time (Lederer and Shirley 1978), with a log (ft) value of 4.1. From Bohr and Mottelson (1969, Vol **1**, p. 410),

$$B(\mathrm{GT}) = \left(\frac{g_A}{g_V}\right)^2 \mathcal{Q}\,|\langle\boldsymbol{\sigma}\rangle|^2_{\mathrm{SM}} \tag{5}$$

$$= \frac{1}{(2J_i+1)}\left(\frac{g_A}{g_V}\right)^2 \mathcal{Q}\,|\langle f\|\,\sigma\tau\,\|\,i\rangle|^2_{\mathrm{SM}} \tag{6}$$

$$= \frac{6250}{ft_{1/2}} \,, \tag{7}$$

where everything is as defined above, times are measured in seconds, and "SM" stands for the value obtained using shell model methods. Note that B(GT) as used in this paper is normalized with respect to the definition given in Bohr and Mottleson (1969), so that our strength is unitless:

$$B_{\mathrm{here}}(\mathrm{GT}) = \frac{4\pi}{G_F^2} B_{\mathrm{BM}}(\mathrm{GT}) \,. \tag{8}$$

For the ^{62}Fe β-decay, J_i is 0. Thus the square of the empirical matrix element is

$$\mathcal{Q}\,|\langle f\|\,\sigma\tau\,\|\,i\rangle|^2 = \frac{6250}{(1.25)^2 ft_{1/2}} \tag{9}$$

$$= 0.3177 \,. \tag{10}$$

Now this β-decay involves one of the four valence neutrons in the ^{62}Fe $1f_{5/2}$ shell going into a $1f_{7/2}$ proton hole (see Fig. 1). In ^{60}Fe there are only two such valence neutrons, so the B(GT) for ^{60}Fe should be half of that for ^{62}Fe (see the Apendix). Thus, the square of the empirical matrix element should be approximately 0.159 for $^{60}\mathrm{Fe} \rightarrow {}^{60}\mathrm{Co} + e^- + \bar{\nu}_e$. Using detailed balance, we divide this by $(2J_i + 1) = 3$ and, using equation (5), can then obtain B(GT) for the electron capture transition.

In the Appendix, we show that the naive shell model number is $|\langle\boldsymbol{\sigma}\rangle|^2_{\mathrm{SM}} = 8/7$. This implies a quenching factor of 0.14, much

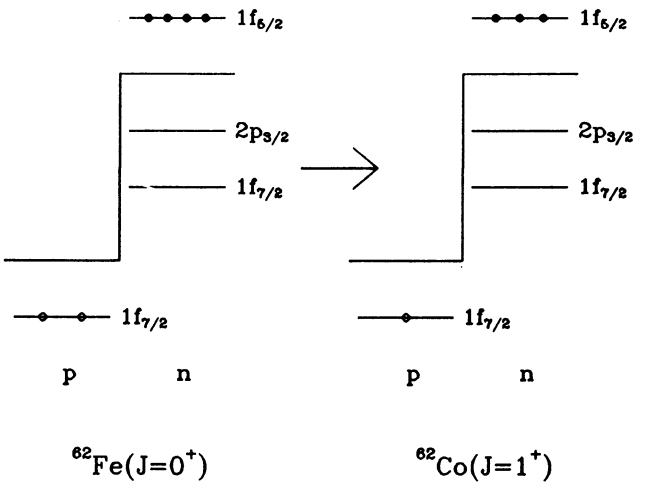

FIG. 1.—The occupation of the not completely filled shells is shown for ^{62}Fe and ^{62}Co nuclei. Solid circles are particles in an otherwise empty shell, while empty circles are holes in an otherwise filled shell. In β-decay, a $1f_{5/2}$ neutron becomes a $1f_{7/2}$ proton. In ^{60}Fe there are only half as many $1f_{5/2}$ neutrons to choose from. Thus from the Appendix, B(GT) is reduced to 1/2 of the strength of the ^{62}Fe transition. In the ^{64}Fe transition, there are 3/2 times as many neutrons to decay. Thus the Appendix predicts that the strength of this transition is 1.5 times larger than ^{62}Fe's.

smaller than those seen in the iron to manganese transition. This is also much smaller than the 0.29 estimated from the energy of the excited 1^+ state in ^{60}Co. Our argument of scaling the B(GT) from the $^{62}\text{Fe} \rightarrow {}^{62}\text{Co}$ β-decay should be reliable, so we do not need to know the quenching factor here, although it is of interest elsewhere.

Now that B(GT) can be determined, we can turn to the phase space integral. It is numerically evaluated using a fourth-order Hammings modified predictor-corrector method (Ralston and Wilf 1960, p. 95; Ralston 1962). However, if $\hat{\mu}^*$ is large, it is possible to obtain analytical approximations for $\langle \epsilon_\nu^2 \rangle$ which are accurate to within roughly 20% for 2×10^9 K $< T < 5 \times 10^9$ K and 1×10^7 g cm^3 $< \rho < 1 \times 10^{10}$ g cm^{-3}. Begin by setting $F(Z, \epsilon_e) = 1$ for now. If $\hat{\mu}^*$ is greater than roughly 2 MeV, the lower limit of the phase space integral ensures that the electrons are relativistic, and we do not error much by replacing p_e by ϵ_e throughout the integral. Also, for the density and temperature regime given above, we can approximate the Fermi-Dirac distribution function by $\exp[(\mu_e - \epsilon_e)/k_B T]$. With these approximations, we obtain the following expression for $\langle \epsilon_\nu^2 \rangle^0$:

$$\langle \epsilon_\nu^2 \rangle^0 = \frac{1}{\pi^2 \rho N_A Y_e} \int_{\hat{\mu}^*}^{\infty} \epsilon_e^2 (\hat{\mu}^* - \epsilon_e)^2 \, d\epsilon_e \exp[(\mu_e - \epsilon_e)/k_B T] . \tag{11}$$

The 0 superscript denotes that this approximation neglects the Fermi function. This expression can now be integrated analytically. The final expression is

$$\langle \epsilon_\nu^2 \rangle^0 = \frac{2.21}{\rho_7 Y_e} \exp\left(\frac{\mu_e - \hat{\mu}}{T}\right) (2T^3 \hat{\mu}^{*2} + 12T^4 \hat{\mu}^* + 24T^5), \tag{12}$$

where all energies and temperatures are in MeV and ρ_7 is the density in 10^7 g cm^{-3}. All that is needed is an analytic expression for μ_e. The electron chemical potential is found by inverting the expression for the lepton number density:

$$n_e = \frac{8\pi}{(2\pi)^3} \int_0^\infty p_e^2 \, dp_e \times \left\{ \left[1 + \exp\left(\frac{\epsilon_e - \mu_e}{K_B T} \right) \right]^{-1} - \left[1 + \exp\left(\frac{\epsilon_e + \mu_e}{k_B T} \right) \right]^{-1} \right\} . \tag{13}$$

In the highly degenerate regime, this expression can be approximated (Bludman and van Riper 1978) by using recursion relations for the relativistic Fermi integrals. In our range of temperature and density, the electrons are not degenerate enough for this approximation to hold. A satisfactory approximation in our regime is given by

$$\mu_e = 1.11(\rho_7 Y_e)^{1/3} \left[1 + \left(\frac{\pi}{1.11} \right)^2 \frac{T^2}{(\rho_7 Y_e)^{2/3}} \right]^{-1/3} , \tag{14}$$

where T is in MeV. This expression is only an approximation of the actual solution of μ_e for highly relativistic electrons. Using this expression in the analytical approximation for the electron capture rates yields capture rates which are fairly close to the numerical results, as will be shown below.

The above integrals computed the electron capture rate as if the electrons interacted with the nucleus as plane waves. Actually, the electron wave functions are distorted by the nuclear Coulomb field. The Fermi function corrects for this. $F(Z, \epsilon_e)$ is defined as $|\psi_{\text{Coulomb}}|^2/|\psi_{\text{free}}|^2$, and, for relativistic electrons, has the form

$$F(Z, \epsilon_e) = 2(1 + \gamma) \left(\frac{2 p_e R}{\hbar} \right)^{-2(1-\gamma)} e^{\pi\nu} \frac{|\Gamma(\gamma + i\nu)|^2}{|\Gamma(2\gamma + 1)|^2} , \tag{15}$$

where ν is $Ze^2/\hbar v_e$, γ is $[1 - (Z\alpha)^2]^{1/2}$, R is the nuclear radius, and Γ is the gamma function. This expression does not include the finite size of the nucleus and is rather laborious to compute. A simple fit to $F(Z, \epsilon_e)$ obtained by Schenter and Vogel (1983). which does include the effect of finite nuclear size, has been used instead. Their fit actually is meant for cases in which the nuclei are not fully ionized, but are still screened by its atomic electrons. Although this is not the case for our nuclei, the correction is small relative to the uncertainties in the matrix elements and energy levels of these nuclei. Schenter and Vogel (1983) find that the Fermi function can be fitted by a simple analytic approximation. This fit is what is used in computing our electron capture rates and β-decay rates. The approximation has the form

$$F(Z, \epsilon_e) = \frac{\epsilon_e}{p_e} \exp\left[\alpha(Z) + \beta(Z) \sqrt{\frac{T}{m_e}} \right] , \tag{16}$$

where $\alpha(Z)$ and $\beta(Z)$ depend upon the nuclear charge Z and the kinetic energy of the electron, T ($T = \epsilon_e - m_e$). They have the following form:

$$\alpha(Z) = -0.881 + 4.46(-2)Z + 1.08(-4)Z^2 \qquad (T < 1.2 m_e) , \tag{17}$$

$$= -8.46(-2) + 2.48(-2)Z + 2.37(-4)Z^2 \qquad (T \geq 1.2 m_e) , \tag{18}$$

$$\beta(Z) = 0.673 - 1.82(-2)Z + 6.38(-5)Z^2 \qquad (T < 1.2 m_e) , \tag{19}$$

$$= 1.15(-2) + 3.58(-4)Z - 6.17(-5)Z_2 \qquad (T \geq 1.2 m_e) . \tag{20}$$

When $\hat{\mu}^*$ is greater than roughly 2 MeV, the electrons which contribute will be fairly highly relativistic. Thus the Fermi function becomes

$$F(Z, \epsilon_e) = \exp\left[\alpha(Z) + \beta(Z)\sqrt{\epsilon_e/m_e}\right] \quad (21)$$

This expression for F will still yield an integral which cannot be expressed as a finite sum of elementary functions.

We can gain an analytical approximation if we form

$$\langle\epsilon_\nu^2\rangle^{\rm C} = \langle\epsilon_\nu^2\rangle^0 \exp\left[\alpha(Z) + \beta(Z)\sqrt{\langle\epsilon_e\rangle/m_e}\right] . \quad (22)$$

The C superscript indicates that we have included Coulomb effects. $\langle\epsilon_e\rangle$ is an average of the electron energy, but a very special kind of average. It is the average over only those electrons which can take part in the capture reaction. Thus we will only average over electrons with energy greater than $\hat{\mu}^*$:

$$\langle\epsilon_e\rangle \approx \frac{\int_{\hat{\mu}^*}^{\infty} \epsilon_e^3 \exp\left[(\mu_e - \epsilon_e)/t\right] d\epsilon_e}{\int_{\hat{\mu}^*}^{\infty} \epsilon_e^2 \exp\left[(\mu_e - \epsilon_e)/t\right] d\epsilon_e} \quad (23)$$

$$\approx \frac{\hat{\mu}^{*3}T + 3\hat{\mu}^{*2}T^2 + 6\hat{\mu}^*T^3 + 6T^4}{\hat{\mu}^{*2}T + 2\hat{\mu}^*T^2 + 2T^3} . \quad (24)$$

Using this expression, one can obtain the average electron energy to put into the expression for $\langle\epsilon_\nu^2\rangle^{\rm C}$.

In Table 1A we have a comparison of all these methods of evaluation with the FFN rates for electron capture on ^{60}Co when Y_e has a value of 0.5. In Table 1B we compare results for the ^{62}Co electron capture rate with those obtained from the Mazurek *et al.* (1974), calculation, also when $Y_e = 0.5$. For the ^{60}Co transition the agreement of the analytical expressions with the numerical results is very poor. At a density of 10^7 g cm^{-3} and a temperature of 3×10^9 K, $\lambda_{\rm an}^0$ is too large by 25% and $\lambda_{\rm an}^{\rm C}$ is too large by 6%. As temperature or density increases, the analytical expressions make estimates which are too large by factors of as much as 4. This is because $\hat{\mu}^*$ is -0.0166 MeV for this transition. This is not the case in which the approximations were meant to apply. Thus only the numerical results can be trusted for this transition. We see that at the lowest density and temperature on the table, FFN obtain a rate which is 10 times our result, $\lambda_{\rm num}^{\rm C}$. This is not surprising because we have computed only the transition from the lowest 1^+ state of ^{60}Co and have used the experimentally obtained quenching factor. FFN did not use this quenching factor and used a full partition function and included all possible transitions. Thus, one expects their rates to become even larger than ours at higher temperatures and densities due to the greater accessibility of excited states. This discrepancy is discussed at greater length in the last section of this paper.

TABLE 1

COMPARISON OF RATES FOR ELECTRON CAPTURE

ρ (g cm^{-2})	Type of Rate	3×10^9 K	4×10^9 K	5×10^9 K
	A. ^{60}Co → ^{60}Fe Electron Capture			
10^7.....	FFN	2.5 (−5)	2.6 (−4)	1.3 (−3)
	$\lambda_{\rm an}^0$	1.99(−6)	6.95(−6)	1.93(−5)
	$\lambda_{\rm num}^0$	1.59(−6)	4.72(−6)	1.14(−5)
	$\lambda_{\rm an}^{\rm C}$	3.82(−6)	1.44(−5)	4.01(−5)
	$\lambda_{\rm num}^{\rm C}$	3.56(−6)	1.03(−5)	2.44(−5)
10^8.....	FFN	1.9 (−3)	8.6 (−3)	2.4 (−2)
	$\lambda_{\rm an}^0$	1.28(−4)	1.59(−4)	2.29(−4)
	$\lambda_{\rm num}^0$	3.17(−5)	7.62(−5)	1.40(−4)
	$\lambda_{\rm an}^{\rm C}$	2.68(−4)	3.30(−4)	4.75(−4)
	$\lambda_{\rm num}^{\rm C}$	6.75(−5)	1.60(−4)	2.91(−4)
	B. ^{62}Co → ^{62}Fe Electron Capture			
10^7.....	Mazurek *et al.*	9.7e(−11)	7.7 (−9)	1.9 (−7)
	$\lambda_{\rm an}^0$	1.42(−8)	3.12(−7)	2.52(−6)
	$\lambda_{\rm num}^0$	1.64(−8)	2.57(−7)	1.67(−6)
	$\lambda_{\rm an}^{\rm C}$	4.28(−8)	6.30(−7)	5.11(−6)
	$\lambda_{\rm num}^{\rm C}$	3.38(−8)	5.21(−7)	3.38(−6)
10^8.....	Mazurek *et al.*	7.0 (−9)	1.8 (−7)	2.4 (−6)
	$\lambda_{\rm an}^0$	8.94(−7)	7.13(−6)	2.99(−5)
	$\lambda_{\rm num}^0$	1.10(−6)	7.73(−6)	2.89(−5)
	$\lambda_{\rm an}^{\rm C}$	1.80(−6)	1.44(−5)	6.04(−5)
	$\lambda_{\rm num}^{\rm C}$	2.25(−6)	1.57(−5)	5.84(−5)

NOTES.—Electron capture rates have been computed in four different ways for comparison with the rates currently used in stellar evolution calculations. The units of each rate are s^{-1}. The superscript "0" indicates that the rate was calculated without including Coulomb effects on the electron wavefunction, while a "C" indicates that these effects were included. The "an" subscript indicates the use of one of the analytical forms discussed in the paper. The "num" subscript indicates that the rate was computed numerically.

In table 1B we see that both analytical approximations are accurate to within 20% for all of the rates computed, except for $\lambda_{\rm an}^{\rm C}$ at $\rho = 10^7$ g cm^{-3} and $T = 5 \times 10^9$ K. Fortunately, the presupernova evolution does not reach such high temperatures at such low densities. In this case we have compared with the Mazurek *et al.* (1974) rates which have been used in recent stellar evolution calculations (Woosley, Pinto, and Weaver 1988), since FFN did not go this high in A. We see that there are severe disagreements between our results and theirs. Even without including all excited states, our rates are typically roughly a factor of 100 larger than their rates. Such a large increase indicates that the underestimate of transitions with nuclei having $A > 60$ might be important.

The time rate of change of Y_e due to a particular transition is given by the following equation:

$$\left.\frac{dY_e}{dt}\right|_i^{(Z,A)} = \mp Y_{(Z,A)}\lambda_i^{(Z,A)} , \quad (25)$$

where the subscript i denotes a transition from the ith excited state of the mother nucleus, $Y_{(Z,A)}$ is the mass fraction per nucleon of the mother nucleus [$Y_{(Z,A)} = X_{(Z,A)}/A$], and $\lambda_i^{(Z,A)}$ is the transition rate from the ith excited state of the (Z, A) nucleus. The plus sign applies for β^--decay, while the minus sign is for electron capture (e.c.) The total rate of change of Y_e due to one nucleus is given by

$$\left.\frac{dY_e}{dt}\right|^{(Z,A)} = Y_{(Z,A)}\left[+\sum_{\beta^-\text{-decay}} \lambda_i^{(Z,A)}(\beta^-) - \sum_{e^-\text{cap}} \lambda_i^{(Z,A)}(\text{e.c.})\right] . \quad (26)$$

We will try to estimate the size of contributions by computing the rate of change of Y_e due to the single transitions we have just calculated.

In Table 2, the mass fractions per nucleon are listed for each mother nucleus for four different values of Y_e at a density of 10^8 g cm^{-3} and two temperatures: 3×10^9 K and 4×10^9 K. In calculating the mass fractions for each nuclear species, we have not included excited states. The abundances obtained are only of heuristic value, since only the ground states are included. We see that for ^{60}Co at $T_9 = 4 \times 10^9$ K,

$$\frac{dY_e}{dt} = -\frac{1.7(-4) \times 1.60(-4)}{60} \text{ s}^{-1} , \quad (27)$$

$$= 4.5(-10) \text{ s}^{-1} . \quad (28)$$

TABLE 2

REACTIONS CONSIDERED

Transition	Y_e^i	Y_e^f	J_{gs}	B(GT)	E_i^{ex}	$\hat{\mu}^*$	$X_p(Y_e = 0.45)$	$X_p(Y_e = 0.44)$	$X_p(Y_e = 0.43)$	$X_p(Y_e = 0.32)$	T_9
$^{60}_{27}Co \rightarrow {}^{60}_{26}Fe$	0.450	0.433	5	0.08274	0.7388	−0.0166	8.8(−4)	1.7(−4)	1.4(−5)	1.5(−7)	4
							7.6(−5)	1.2(−5)	5.8(−7)	4.8(−10)	3
$^{62}_{27}Co \rightarrow {}^{62}_{26}Fe$	0.435	0.419	2	0.16548	0.5061	2.575	7.6(−6)	2.2(−4)	2.0(−4)	2.7(−5)	4
							2.0(−7)	1.6(−5)	1.4(−5)	6.4(−7)	3
$^{64}_{27}Co \rightarrow {}^{64}_{26}Fe$	0.422	0.406	1	0.24823	0	4.411	1.4(−9)	6.1(−6)	6.3(−5)	1.1(−4)	4
							3.1(−12)	1.2(−7)	2.0(−6)	4.8(−6)	3
$^{66}_{29}Cu \rightarrow {}^{66}_{28}Ni$	0.439	0.424	1	0.13145	0	0.747	3.5(−6)	2.9(−5)	1.3(−5)	7.1(−7)	4
							1.3(−7)	2.2(−6)	8.3(−7)	9.0(−9)	3
$^{67}_{29}Cu \rightarrow {}^{67}_{28}Ni$	0.433	0.418	3/2	0.395	0	4.341	1.8(−5)	1.8(−3)	2.8(−3)	5.4(−4)	4
							1.2(−6)	4.4(−4)	7.2(−4)	5.7(−5)	3
$^{68}_{29}Cu \rightarrow {}^{68}_{28}Ni$	0.426	0.412	1	0.787	0	3.081	1.7(−8)	2.0(−5)	1.0(−4)	7.1(−5)	4
							1.2(−10)	1.0(−6)	7.2(−6)	4.2(−6)	3
$^{70}_{29}Cu \rightarrow {}^{70}_{28}Ni$	0.414	0.400	1	1.574	0	4.671	3.4(−13)	6.1(−8)	3.5(−6)	3.0(−5)	4
							8.0(−17)	3.4(−10)	4.4(−8)	1.4(−6)	3
$^{69}_{30}Zn \rightarrow {}^{69}_{29}Cu$	0.435	0.420	1/2	0.125	0	2.991	1.8(−7)	9.9(−6)	1.0(−5)	1.3(−6)	4
							3.9(−9)	6.8(−7)	7.2(−7)	2.8(−8)	3
$^{60}_{27}Co \rightarrow {}^{60}_{28}Ni$	0.450	0.467	5	1.0324	0.7388	−4.074	8.8(−4)	1.7(−4)	1.4(−5)	1.5(−7)	4
							7.6(−5)	1.2(−5)	5.8(−7)	4.8(−10)	3
$^{62}_{27}Co \rightarrow {}^{62}_{28}Ni$	0.435	0.452	2	0.6882	0.5061	−6.332	7.6(−6)	2.2(−4)	2.0(−4)	2.7(−5)	4
							2.0(−7)	1.6(−5)	1.4(−5)	6.4(−7)	3
$^{63}_{27}Co \rightarrow {}^{62}_{28}Ni$	0.429	0.444	7/2	0.09649	0	−4.086	7.7(−6)	2.7(−3)	8.2(−3)	3.9(−3)	4
							1.9(−7)	3.3(−4)	1.3(−3)	4.2(−4)	3
$^{64}_{27}Co \rightarrow {}^{64}_{28}Ni$	0.422	0.438	1	0.3441	0	−7.818	1.4(−9)	6.1(−6)	6.3(−5)	1.1(−4)	4
							3.1(−12)	1.2(−7)	2.0(−6)	4.8(−6)	3

NOTES.—All relevant information for the electron capture and β-decay transitions discussed in this paper are listed. The second and third columns list Z/A for the parent and daughter nuclei, respectively. J_{gs} is the spin of the ground state. B(GT) is the Gamow-Teller strength of the particular transition. E_i^{ex} is the energy in MeV of the initial state, measured from the ground state. "0" means we are using the ground state; $\hat{\mu}$ is as defined in the paper. The last four columns list the abundance of the ground state of each nucleus at $\rho = 10^8$ g cm^{-3}, and the temperature and value of Y_e listed.

This is very small, even when multiplied by the Kelvin-Helmholtz contraction time of $\sim 4 \times 10^5$ s following silicon burning. However, we know from the output of the stellar evolution calculation of Woosley, Pinto, and Weaver (1988) that this reaction gives roughly half of the electron capture of $Y_e \sim 0.43 \times 10^8$ g cm^{-3} is the density at which significant electron capture begins. Densities do become larger as time goes by.

In Figure 2, the temporal evolution of central density and central temperature are shown for an 18 $M_\odot$ star (Woosley, Pinto, and Weaver 1988) during and after silicon burning. This figure gives a general idea of the temperatures and densities seen. The Kelvin-Helmholtz contractions we have been discussing occur after the completion of silicon core burning and after the oxygen shell burning shown on the plot. It can be seen that densities do exceed 10^8 during these contractions. Were we to use $\rho_8 = 3$ in our estimates, λ, and thus dY_e/dt would be an order of magnitude larger. In any case, these rates will be put into stellar evolution codes to see exactly what their effects are.

If one refers to the analytical approximations for λ one sees that its behavior is dominated by a particular factor:

$$\lambda \sim \exp\left[-\frac{(\hat{\mu}^* + \Delta^*)}{k_B T}\right]\hat{\mu}^{*2} . \quad (29)$$

The exponentiated factor is the difference in energy between the two ground states of the nuclei. The nuclei with the largest electron capture rates will be those with the smallest "wall" to climb. In the next section, we discuss several such nuclei.

III. THE Cu + e^- → Ni ELECTRON CAPTURE RATES

^{67}Ni β-decays from a particularly simple neutron $2p_{1/2}$ state to ^{67}Cu with a proton in the $2p_{3/2}$ state (see Fig. 3). This transition is from a ground state to a ground state and the log (ft) value has been measured (Reiter, Breunlich, and Hille 1975) at 4.5. This gives a B(GT) of 0.198 and

$$\mathcal{2}|\langle f \| \sigma\tau \| i\rangle^2 = 0.1265 . \quad (30)$$

If one computes (de Shalit and Talmi 1963, p. 57) the reduced matrix element for a one particle transition using a naive shell model, one obtains

$$|\langle f \| \sigma\tau \| i\rangle|^2_{NSM} = \frac{8}{3} , \quad (31)$$

giving a quenching factor of 0.05, much smaller than we obtained for the Co → Fe transitions.

As is seen in table 2, the B(GT) for the inverse reaction is twice what we just computed, because of detailed balance. Thus it is slightly larger than ^{60}Co → ^{60}Fe strength. Using the method of Appendix A to find transition strengths for ^{68}Cu and ^{70}Cu, we obtain strengths which are 2 and 4 times, respectively, as large as for ^{67}Cu. The Gamow-Teller strength of electron capture upon ^{66}Cu has been determined separately using its own inverse reaction ft-value, listed in Lederer and Shirley (1978).

Table 3 lists rates of electron capture on ^{66}Cu, ^{67}Cu, and ^{68}Cu. The first nucleus provides the largest capture rate, 3.45(−3) s^{-1}. But its maximal abundance (see Table 2) is less by a factor of 10 than either of the two heavier copper nuclei. For this nucleus, we find that over the contraction time of 4×10^5 s the change in Y_e is roughly 0.0006 for $\rho_8 = 1$. ^{67}Cu is 200 times more abundant, but its capture rate is roughly 1000 times slower. For this nucleus we obtain $\Delta Y_e \sim 6(-5)$. For ^{68}Cu, the change in Y_e will be 1(−4). All of these rates are calculated at a density of 10^8 g cm^{-3}. The other nuclei listed in Table 2 yield rates that are of this same order. In these cases,

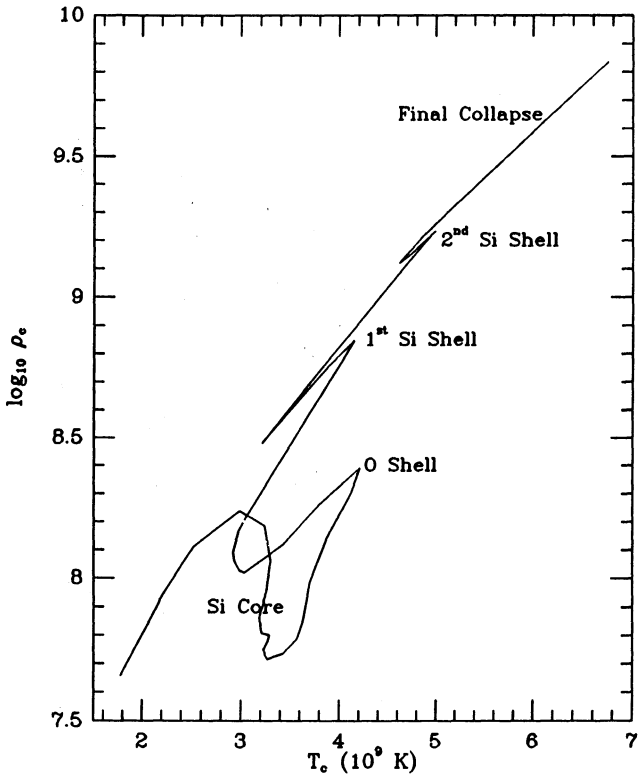

FIG. 2.—The $\log_{10}$ of central density vs. central temperature is plotted as a function of time for the developing iron core. The plot begins in the lower left corner with the silicon core contracting toward central silicon ignition. The plot ends in the upper right corner with the fully developed iron core in its final collapse stage. Each major burning stage which affects the core is listed. The core burning lasts for 5.1 days. From the end of core burning to the end of O shell burning is another 4.7 days. From the end of O shell burning to the end of the first Si shell burn is 2.5 more days. 2.2 days is spent in the contraction before this shell ignites. The rest of the evolution on the plot takes only 38 minutes.

electron capture is small unless the density is substantially higher that $\rho_8 = 1$, or unless excited states contribute substantially.

IV. β-DECAYS OF ^{64,63,62,60}Co

Given typical Kelvin-Helmholtz contraction times on the order of 4×10^5 s, it is surprising to see the β-decay half-life of ^{64}Co of 0.30 ± 0.03 s (Rahkonen and Kantele 1974). At present, this decay has not been included in the stellar evolution calculations of Weaver and Woosley. Of course, this half-life was measured in an environment not immersed in a sea of degenerate electrons. The half-life will be somewhat increased because of blocking. Using Fermi's golden rule, it can be shown that the decay rate can be expressed in a form analogous to that for electron capture:

$$\lambda = \frac{G_F^2}{2\pi^3} B(\mathrm{GT}) \frac{(2J_i^{\mathrm{ex}} + 1)}{Z_n} \exp\left(\frac{-E_i^{\mathrm{ex}}}{k_B T}\right) \times \int_0^{\sqrt{\hat{\mu}^{*2} - m_e^2}} \frac{p_e^2(\hat{\mu}^* + \varepsilon_e)^2 F(Z, \epsilon_e)\, dp_e}{1 + \exp\left[(\mu_e - \epsilon_e)/k_B T\right]} . \quad (32)$$

All factors are as they have been defined throughout the paper. One can estimate the effect of blocking on the decay rate by computing a blocking factor F:

$$F \simeq 1 - 10\left(\frac{\mu_e}{-\hat{\mu}^*}\right)^3 , \quad (33)$$

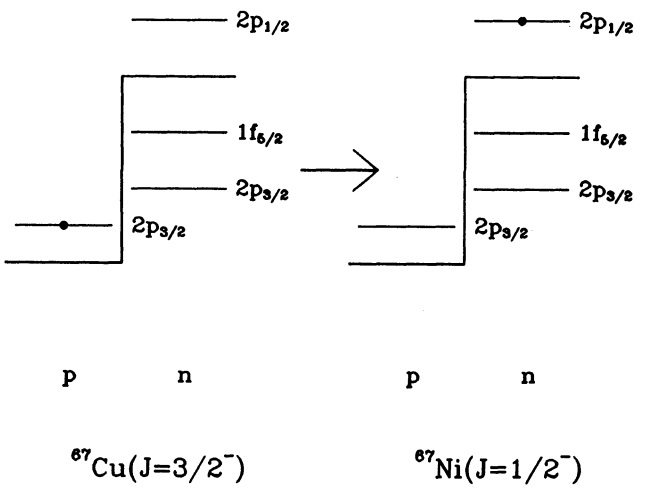

FIG. 3.—The electron capture shown involves a single particle transition from the $2p_{3/2}$ shell to the $2p_{1/2}$ shell. The method of the Appendix is used to computed the matrix elements for ^{68}Cu and ^{70}Cu.

where $\mu_e \ll -\hat{\mu}^*$. For this reaction $\hat{\mu}^*$ is -7.818 MeV. At $T = 4 \times 10^9$ K, $\rho = 10^8$ g cm^{-3}, and $Y_e = 0.45$, μ_e has a value of 1.8 MeV. The blocking factor then becomes

$$F \simeq 1 - 10(1.8/7.818)^3 \quad (34)$$

$$\simeq 0.88 \quad (35)$$

which predicts that the half-life should increase to roughly 0.34 s, still very small compared with the Kelvin-Helmholtz time. In Table 4A, the β-decay rates have been computed numerically and are listed in the same format as the Table 3 electron capture rates. From this table, we see that at 10^8 g cm^3 and 4×10^9 K the decay rate is 2.09 s^{-1}. Thus the half life will actually be 0.33 s. The blocking factor slighly overestimates the reduction in the rate due to the electron Fermi sea.

The β-decay rates are on the order of two per second and abundances of ^{64}Co (see Table 2) are $\sim 6 \times 10^{-6}$ for $Y_e = 0.44$ and 6×10^{-5} for $Y_e = 0.43$ at a density of 10^8 and temperature of 4×10^9 K. Thus, in a Kelvin-Helmholtz time of 4×10^5 s, there would be roughly four ^{64}Co decays per nucleus in the core of the star for Y_e of 0.44 and roughly 40 for Y_e of 0.43.

In Tables 4B–D, the rates are given for decays of ^{63}Co, ^{62}Co, and ^{60}Co. Note that these rates are 130, 11, and 400 times smaller than those for ^{64}Co. This is because of the dwindling

TABLE 3

ELECTRON CAPTURE RATES

ρ(g cm^{-2})	3×10^9 K	4×10^9 K	5×10^9 K
A. Rates for ^{66}Cu → ^{66}Ni Electron Capture			
10^7.....	8.35(−5)	1.66(−4)	3.23(−4)
10^8.....	2.64(−3)	3.45(−3)	4.56(−3)
B. Rates for ^{67}Cu → ^{67}Ni Electron Capture			
10^7.....	2.45(−9)	1.22(−7)	1.56(−6)
10^8.....	1.66(−7)	3.71(−6)	2.73(−5)
C. Rates for ^{68}Cu → ^{68}Ni Electron Capture			
10^7.....	3.72(−7)	5.64(−6)	3.59(−5)
10^8.....	2.50(−5)	1.72(−4)	6.25(−4)

NOTES.—$\lambda^{\mathrm{C}}_{\mathrm{num}}$ has been computed as a function of temperature and density of Y_e of 0.5. The units of each rate are s^{-1}.

TABLE 4

DECAY RATES

A. Rates for ^{64}Co → ^{64}Ni β-Decay			
10^7.....	2.27	2.27	2.27
10^8.....	2.08	2.09	2.09
B. Rates for ^{63}Co → ^{63}Ni β-Decay			
10^7.....	2.42(−2)	2.43(−2)	2.43(−2)
10^8.....	1.53(−2)	1.60(−2)	1.69(−2)
C. Rates for ^{62}Co → ^{62}Ni β-Decay			
10^7.....	1.34(−1)	2.19(−1)	2.93(−1)
10^8.....	1.14(−1)	1.89(−1)	2.55(−1)
D. Rates for ^{60}Co → ^{60}Ni β-Decay			
10^7.....	3.97(−3)	8.15(−3)	1.26(−2)
10^8.....	2.49(−3)	5.36(−3)	8.70(−3)

NOTES.—The β-decay rate has been computed as a function of temperature and density for $Y_e = 0.5$. Coulomb corrections have been included in the calculation. Note the extremely weak temperature dependence for the ^{64}Co decay. This happens because of the extremely large $\hat{\mu}^*$ of the decay. The units of each rate are s^{-1}.

though some of the electron capture rates discussed in the previous sections were 2 orders of magnitude larger that those used in current stellar evolution codes, there is not likely to be

current results of Woosley, Pinto, and Weaver (1988).

The β-decay rates from the other cobalt isotopes to nickel isotopes are also rapid, and must be included also. But none compete with the ^{64}Co and ^{63}Co β-decay rate. For example, ^{70}Cu has a 5 s β-decay with a Q-value of 6.17 MeV. However, from Table 2, it can be seen that the ^{70}Cu abundance becomes equal to that of ^{64}Co only for the smallest values of Y_e, 0.41, so the ^{70}Cu will be of only marginal importance in cooling the core.

Note that in the case of β-decays there is less uncertainty about the contributions from excited states than in the case of electron capture. This is because, in the former case, the collective Gamow-Teller strength lies very high above the daughter ground state and thus does not contribute much of its strength at these low temperatures, while in the latter case, this resonance lies much closer to the daughter state and can possibly contribute more strength at low temperatures (FFN 1982*a*). This feature also makes it more difficult to use a shell model to calculate low-energy transition strengths for β-decays because so little strength resides at low daughter energies. We have avoided this problem for now by using experimentally measured transitions

roughly 2 orders of magnitude larger. It is clear that for densities near 10^8 g cm^{-3}, the decay of ^{63}Co, all by itself, will prevent decreases of Y_e below 0.44. The density must increase considerably before the electron capture predominates over the β-decay.

Of course, what will happen when the rapid cobalt β-decays are included is that the temperature will start to decrease, cutting off the abundances of the odd-odd ^{60}Co, ^{62}Co, and ^{64}Co, and of the odd-even ^{63}Co. The abundances will then be concentrated in the even-even nuclei. From the cobalt abundances in Table 2 this can be seen in the transition from temperatures of 4×10^9 K to 3×10^9 K. In each case, the abundance drops by a factor of at least 10. If the temperature drops further, so will the abundances, cutting off the β-decays in dynamical times of several times 10^5 s. We consequently believe that the electron fraction will not drop below 0.44 until later in the contraction, possibly not until collapse. This is larger than the central electron fractions just before collapse in the present calculations and would appear to increase the size of the core, which scales as Y_e^2.

However, one can also show that the electron pressure is proportional to

$$1 + \frac{2}{3}\left(\frac{\pi T}{\mu_e}\right)^2 \tag{39}$$

for relativistic electrons. Thus, in reducing the temperature of the material, these β-decays will also reduce the ability of the core to support itself. Clearly these effects will find some balance. This balance might or might not lead to substantially different post-core-silicon-burning behavior. The only way we will know for sure is by incorporating these rates into the stellar evolution code.

From Table 1A it was seen that the rates calculated for the $^{60}\text{Co} \rightarrow {}^{60}\text{Fe}$ electron capture are smaller than those of FFN (1982*a*) by more than an order of magnitude. Part of this is because we have included a rather small quenching factor of $\frac{1}{2}$ obtained from relating the $^{60}\text{Co} \rightarrow {}^{60}\text{Fe}$ transition to the ^{62}Fe β-decay.

We have included only the lowest excited 1^+ state in ^{60}Co in our calculation, making a shell model calculation in which the angular momentum recoupling also gave a rather small factor. The calculations of FFN (1982*a*) obtain large contributions from more highly excited states. We are presently trying to estimate such contributions from large shell model calculations, but at the present the results are very uncertain. Possibly it is better to obtain information from (*n*, *p*) experiments. Unfortunately, they cannot presently be done on the ^{60}Co state, which is an excited state.

However, very detailed (*n*, *p*) experiments have been performed on ^{54}Fe (Vetterli *et al.* 1989). The main transition here is to the 1^+ excited state in ^{54}Mn at 1.45 MeV. In the naive shell model, this involves the same $f_{7/2}$ proton to $f_{5/2}$ neutron transition as in ^{60}Co, although the recoupling coefficients are different. In the $^{54}\text{Fe}(n, p)^{54}\text{Mn}$ reaction (Vetterli *et al.* 1989) substantial strength is found in excited states, but when multiplied by Boltzmann factors for T_9 of 3 to 4, this would increase the strength from the lowest 1.45 MeV state by less than a factor of 2. On the basis of the low temperatures we expect, we do not think our electron capture will be increased by a large factor upon the inclusion of excited states, although we will work further on this problem. Increased electron capture would only help in establishing our conjectured scenario, because it would more rapidly reduce Y_e to the neutron-rich region where the cobalt β-decays begin.

Data on (*n*, *p*) reactions are presently accumulating, and much more is known about quenching factors than when Fuller and collaborators performed their calculations, so it clearly will be worthwhile to redo their calculations, and we plan to do this. The new (*n*, *p*) data from TRIUMF is mostly still in the analysis stage. It should give us good indications about the amount of strength in excited states, which we have not included. Furthermore, extensive shell model calculations will be helpful in estimating these strengths. However, if the rapid β-decays keep the core cool, these excited states may not contribute much.

We would like to thank Stan Woosley and Tom Weaver for helpful discussions and access to their stellar evolution calculations, George Fuller for many useful insights into how weak interaction rates have been calculated for stellar evolution codes, and Ed Baron and Jerry Cooperstein for many useful discussions. This work was supported in part by the US Department of Energy under contract DE-AC02-76CH00016, and grants DE-FG02-88ER40388 and DE-FG02-88ER40397.

APPENDIX A

For ease of calculation, we derive a general formula for $0^+ \rightarrow 1^+$ even-even to odd-odd weak interaction transitions. The shell structure for other transitions are more complicated and need to be considered on an individual basis. To be specific, we consider here β-decay. From Bohr and Mottelson (1969, Vol. **1**, p. 410), we have

$$fT_{1/2} = \frac{1}{B(\text{GT})} \times (6250 \text{ s}) , \tag{A1}$$

where

$$B(\text{GT}) = \frac{1}{(2I_i + 1)} |\langle J_f \| \sigma\tau \| J_i \rangle|^2 \left(\frac{g_A}{g_V}\right)^2 . \tag{A2}$$

We take our initial state to consist of a closed core with n_n valence neutron particle pairs in the j_n-shell and n_p proton hole pairs in the j_p-shell. In this language, ^{62}Fe is considered to be a two-neutron particle pair one-proton hole pair state. Our general even-even initial state is thus written

$$|(j_n^2)^{n_n}_{0^+}(\tilde{j}_p^2)^{n_p}_{0^+} J = 0^+\rangle , \tag{A3}$$

where the tilde ($\sim$) reminds that these are proton *hole* states. Our final state is likewise

$$|(j_n^2)_{0^+}^{n_n-1}(\tilde{j}_p^2)_{0^+}^{n_p-1}(j_n\tilde{j}_p)_{1+M_f}\rangle\,. \tag{A4}$$

Using the language of second quantization we can write the final state as

$$B^\dagger(j_n, j_p\,; 1M_f)|(j_n^2)_{0^+}^{n_n-1}(\tilde{j}_p^2)_{0^+}^{n_p-1}\rangle\,, \tag{A5}$$

where

$$B^\dagger(j_n, j_p\,; \lambda\mu) \equiv \sum_{m_n m_p} C^{j_n\, j_p\, \lambda}_{m_n -m_p \mu}(-1)^{j_p - m_p} a_{j_n m_n} a^\dagger_{j_p m_p}\,. \tag{A6}$$

By definition, a one-body operator is

$$\hat{X}^\lambda_\mu = \sum_{\substack{j_1\, m_1\\ j2\, m2}} \langle j_1\, m_1\,|\, X^\lambda_\mu\,|j_2\, m_2\rangle a^\dagger_{j_1 m_1}\, a_{j_2 m_2}\,. \tag{A7}$$

With this definition and a little angular momentum algebra, we find

$$\hat{\sigma}_\mu = \sum_{j_1\, j_2} \frac{(-1)^{j_1 - j_2 - \mu}}{\sqrt{3}} \langle j_1 \,\|\, \sigma \,\|\, j_2\rangle B(j_1 j_2\, 1 - \mu)\,. \tag{A8}$$

We now put it all together. From our definition of reduced matrix elements, we have

$$\langle \Psi_f \,\|\, \sum_k \tau\sigma(k) \,\|\, \Psi_i\rangle = \sqrt{3}\langle \Psi_f\, 1^+ M_f\,|\,\tau\hat{\sigma}_\mu\,|\,\Psi_i\, 0^+\rangle\,. \tag{A9}$$

Inserting equation (A8) into the right-hand side of equation (A9) and using the fact that equation (A9) is independent of μ, we have

$$\langle \Psi_f \,\|\, \sum_k \tau\sigma(k) \,\|\, \Psi_i\rangle = \frac{1}{\sqrt{3}} \langle j_p \,\|\, \sigma \,\|\, j_n\rangle \langle (j_n^2)_{0^+}^{n_n-1}(\tilde{j}_p^2)_{0^+}^{n_p-1}\,|\,[B(j_n, j_p\,; 1)B(j_n, j_p\,; 1)]^0\,|\,(j_n^2)_{0^+}^{n_n}(\tilde{j}_p^2)_{0^+}^{n_p}\rangle\,, \tag{A10}$$

where

$$[B(j_n, j_p\,; 1)B(j_n, j_p\,; 1)]^0 \equiv \sum_M C^{1\,1\,0}_{M\,-M\,0} B(j_n, j_p\,; 1M)B(j_n, j_p\,; 1 - M)\,. \tag{A11}$$

Note that the τ operator does not directly appear in this formula, as its only role is to change a neutron into a proton.

These zero-coupled operators are easily transformed via the renormalized nine-j symbol i.e.,

$$[B(j_n, j_p\,; 1)B(j_n, j_p\,; 1)]^0 = X\begin{pmatrix} j_p & j_p & 0\\ j_n & j_n & 0\\ 1 & 1 & 0\end{pmatrix} A(j_n, j_n\,; 0)A^\dagger(j_p, j_p\,; 0)\,, \tag{A12}$$

where $A^\dagger(j_1, j_2\,; JM)$ is the two-particle creation operator

$$A^\dagger(j_1, j_2\,; JM) \equiv \sum_{m_1\, m_2} C^{j_1\, j_2\, J}_{m_1\, m_2\, M} a^\dagger_{j_1,\, m_1}\, a^\dagger_{j_2,\, m_2}\,. \tag{A13}$$

Inserting equation (A12) into equation (A10) and using the fact that

$$X\begin{pmatrix} j_p & j_p & 0\\ j_n & j_n & 0\\ 1 & 1 & 0\end{pmatrix} = \frac{\sqrt{3}}{\sqrt{2j_n + 1}\sqrt{2j_p + 1}}\,, \tag{A14}$$

along with

$$\langle (j_n^2)_{0^+}^{n_n-1}(\tilde{j}_p^2)_{0^+}^{n_p-1}\,|\,A(j_n, j_n\,; 0)A^\dagger(j_p, j_p\,; 0)\,|\,(j_n^2)_{0^+}^{n_n}\,(\tilde{j}_p^2)_{0^+}^{n_p}\rangle = 2\sqrt{n_n}\sqrt{n_p}\,, \tag{A15}$$

we obtain the rather simple and intuitively appealing result

$$\left|\left\langle \Psi_f \,\middle\|\, \sum_k \tau\sigma(k) \,\middle\|\, \Psi_i\right\rangle\right|^2 = |\langle j_p \,\|\, \sigma \,\|\, j_n\rangle|^2 \frac{2n_n}{2j_n + 1}\frac{2n_p}{2j_p + 1}\,. \tag{A16}$$

We might prefer to express the result in terms of particle numbers, in which case the previous expression becomes

$$\left|\left\langle \Psi_f \,\middle\|\, \sum_k \tau\sigma(k) \,\middle\|\, \Psi_i\right\rangle\right|^2 = |\langle j_p \,\|\, \sigma \,\|\, j_n\rangle|^2 \frac{N_n}{2j_n + 1}\left(1 - \frac{N_p}{2j_p + 1}\right), \tag{A17}$$

where N_n and N_p are the number of neutrons and protons within the j_n and j_p shells, respectively. This result is a generalization of that found by Towner (1985), and reduces to his formula.

We thus see that our final result under the seniority assumption is intuitively appealing. The full transition rate is simply the

TABLE 5

SINGLE-PARTICLE REDUCED MATRIX ELEMENT

		$\lvert\langle j_f \lVert \sigma \rVert j_i\rangle\rvert^2$	
j_f	j_i	$l+\frac{1}{2}$	$l-\frac{1}{2}$
$l+\frac{1}{2}$	...	$\frac{2(l+1)(2l+3)}{2l+1}$	$\frac{8l(l+1)}{2l+1}$
$l-\frac{1}{2}$	...	$\frac{8l(l+1)}{2l+1}$	$\frac{2l(2l-1)}{2l+1}$

single-particle transition rate multiplied by the probability of having a neutron particle in the shell j_n and the probability of having an unoccupied proton state in the shell j_p.

To achieve the numerical result, we still need to know the single-particle reduced matrix element $\langle j_f \lVert \sigma \rVert j_i\rangle$. This is readily done with angular momentum algebra in Table 5.

REFERENCES

Bertsch, G., and Hamamoto, I. 1983, *Phys. Rev. C*, **26**, 1323.
Bethe, H. A., Brown, G. E., Applegate, J., and Lattimer, J. 1979, *Nucl. Phys. A*, **234**, 487.
Bloom, S. D., and Fuller, G. M. 1985, *Nucl. Phys. A*, **440**, 511.
Bludman, S. A., and van Riper, K. A. 1978, *Ap. J.*, **224**, 631.
Bohr, A., and Mottelson, B. M. 1969, *Nuclear Structure*, Vol. 1. (New York: Benjamin).
———. 1981, *Phys. Letters, B*, **100B**, 10.
Brown, G. E. 1971, *Unified Theory of Nuclear Models and Forces* (Amsterdam: North-Holland).
Brown, G. E., and Rho, M. 1981, *Nucl. Phys, A*, **372**, 397.
de Shalit, A., and Talmi, I. 1963, *Nuclear Shell Theory* (New York: Academic).
Fuller, G. M., Fowler, W. A., and Newman, M. J. 1980, *Ap. J. Suppl.*, **42**, 447.
———. 1982*a*, *Ap. J.*, **252**, 715.
———. 1982*b*, *Ap. J. Suppl.*, **48**, 279.
———. 1985, *Ap. J.*, **293**, 1.
Häuser, O., and Vetterli, M. C. 1988, *Nucl. Phys. A*, **478**, 559.
Lederer, C. M., and Shirley, V. S. 1978, *Table of Isotopes* (7th ed.; New York: John Wiley).
Mazurek, T. J., Cameron, A. G. W., and Truran, J. 1974, *Ap. Space Sci.*, **27**, 261.
Rahkonen, V., and Kantele, J. 1974, *Physica Finnica*, **9**, 103.
Ralston, A. 1962, *Math Comput.*, **16**, 431.
Ralston, A., and Wilf, H. S. 1960, *Mathematical Methods for Digital Computers* (New York: Wiley).
Reiter, W. L., Breunlich, W. H., and Hille, P. 1975, *Nucl. Phys. A*, **249**, 166.
Schenter, G. K., and Vogel, P. 1983, *Nucl. Sci. Eng.*, **83**, 393.
Towner, I. S. 1985, *Nucl. Phys. A*, **444**, 402.
Vetterli, M. C., *et al.* 1989, *Phys. Rev. C*, **40**, 559.
Woosley, S. E., and Hoffman, R. D. 1986, *Tables of Reaction Rates for Nucleosynthesis for Charged Particle and Weak Interactions*, unpublished.
Woosley, S. E., Pinto, P. A., and Weaver, T. A. 1988, *Recent Results on SN 1987A*, preprint.

M. B. AUFDERHEIDE, G. E. BROWN, T. T. S. KUO, and D. B. STOUT: Department of Physics, SUNY, Stony Brook, NY 11794-3800

P. VOGEL: Department of Physics, California Institute of Technology, Pasadena, CA 91125